Electronic Supplementary Information for Dalton Transactions

Supporting information for

Monomeric, dimeric and 1D chain polymeric copper(II) complexes of a pyrrole-containing tridentate Schiff-base ligand and its 4-brominated analogue

Rongqing Li,[a] Boujemaa Moubaraki,[b] Keith S. Murray,[b] and Sally Brooker*[a]

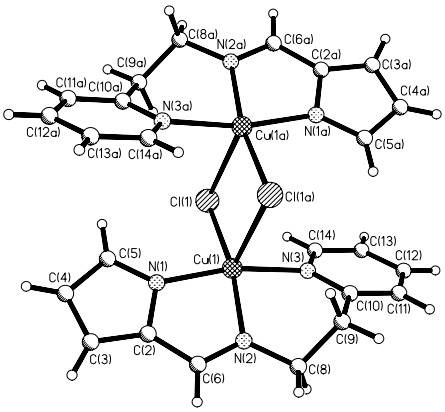

Figure S1. Perspective view of the dimeric copper(II) complex $[Cu_2(L^1)_2(\mu\text{-}Cl)_2]$ (**1**). Symmetry operation a is 1-x, -y, 1-z.

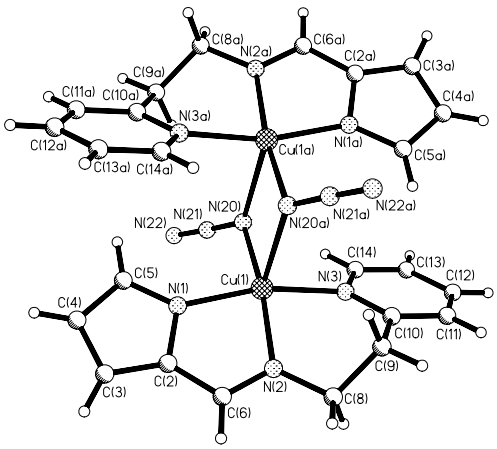

Figure S2. Perspective view of the dimeric copper(II) complex $[Cu_2(L^1)_2(\mu_{1,1}\text{-}N_3)_2]$ (purple prism crystals of **3**). Symmetry operation a is -x, 1-y,-z+1.

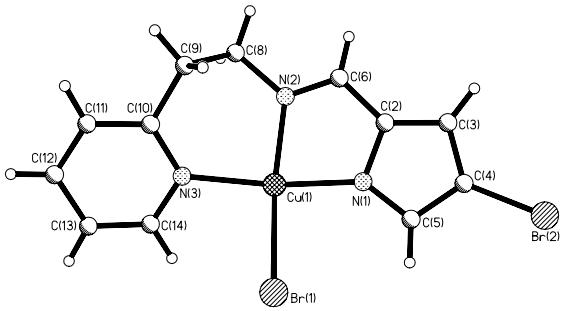

Figure S3. Perspective view of the repeating unit, $[CuL^{1a}Br]$, of the polymeric copper(II) chain complex $[CuL^{1a}(\mu\text{-}Br)]_\infty$ (**5**) showing the atom labelling.

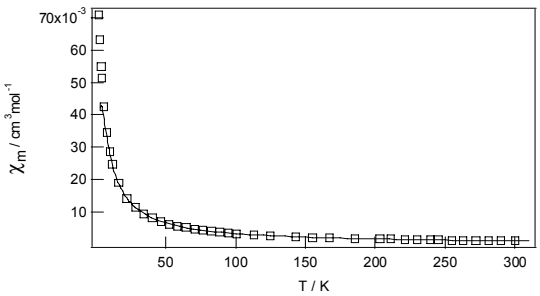

Figure S4. Temperature dependence of the magnetic susceptibility, χ_M, of $[Cu_2(L^1)_2(\mu\text{-}Cl)_2]$ (**1**). The solid line is the best-fit calculated using the parameters given in Table 4.

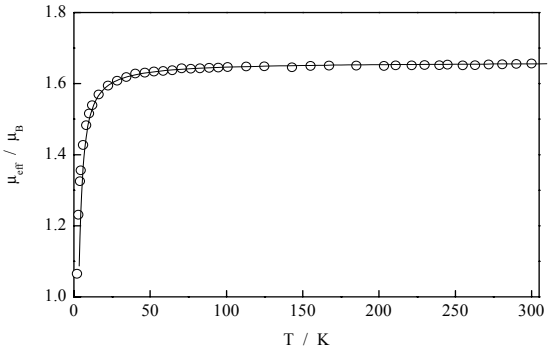

Figure S5. Temperature dependence of the magnetic moment, μ_{eff}, of $[Cu_2(L^1)_2(\mu\text{-}Cl)_2]$ (**1**). The solid line is the best-fit calculated using the parameters given in Table 4.

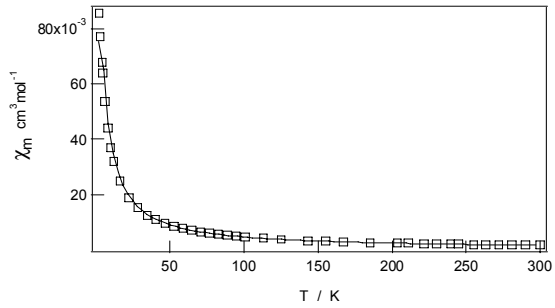

Figure S6. Temperature dependence of the magnetic susceptibility, χ_M, of $[Cu_2(L^1)_2(\mu\text{-}Br)_2]$ (**2**). The solid line is the best-fit calculated using the parameters given in Table 4.

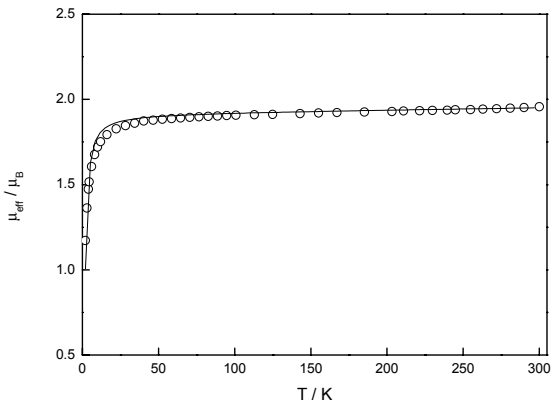

Figure S7. Temperature dependence of the magnetic moment, μ_{eff}, of $[Cu_2(L^1)_2(\mu\text{-}Br)_2]$ (**2**). The solid line is the best-fit calculated using the parameters given in Table 4.

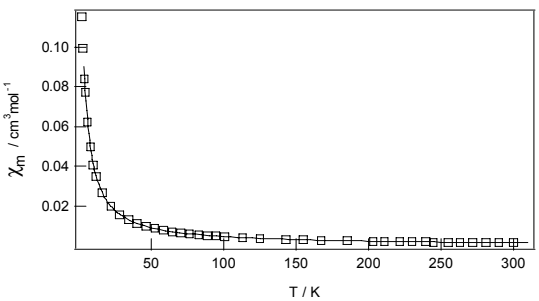

Figure S8. Temperature dependence of the magnetic susceptibility, χ_M, of $[Cu_2(L^1)_2(\mu_{1,1}\text{-}N_3)_2]$ (**3**). The solid line is the best-fit calculated using the parameters given in Table 4.

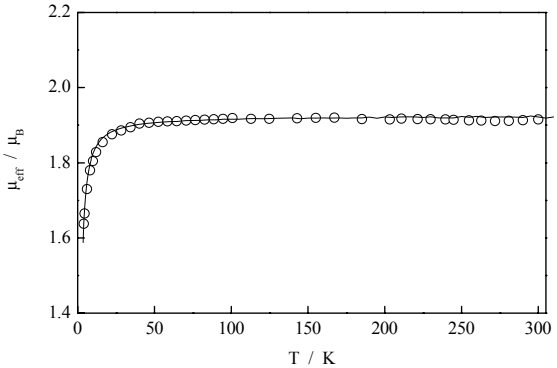

Figure S9. Temperature dependence of the magnetic moment, μ_{eff}, of $[Cu_2(L^1)_2(\mu_{1,1}\text{-}N_3)_2]$ (**3**). The solid line is the best-fit calculated using the parameters given in Table 4.

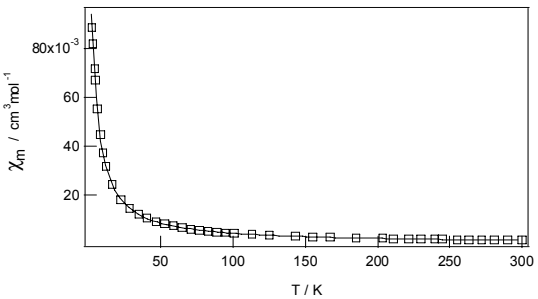

Figure S10. Temperature dependence of the magnetic susceptibility, χ_M, of $[CuL^{1a}(\mu\text{-}Br)]_\infty$ (**5**). The solid line is the best-fit calculated using the parameters given in Table 4.

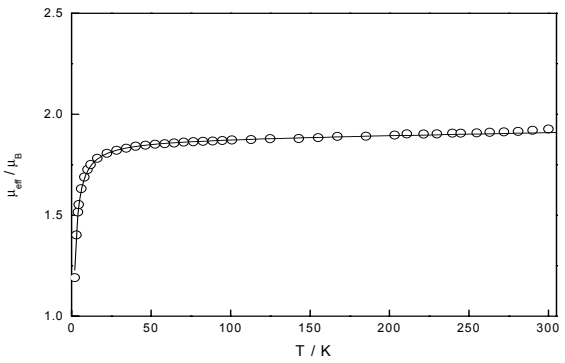

Figure S11. Temperature dependence of the magnetic moment, μ_{eff}, of $[CuL^{1a}(\mu\text{-}Br)]_\infty$ (**5**). The solid line is the best-fit calculated using the parameters given in Table 4.

Table S1 Selected bond lengths [Å] and angles [°] for $[Cu_2(L^1)_2(\mu\text{-}Cl)_2]$ (**1**) and $[Cu_2(L^1)_2(\mu\text{-}Br)_2]$ (**2**).

	X = Cl[b]	**X = Br**
Cu(1)-N(1)	2.0	1.974(2)
Cu(1)-N(2)	2.0	2.017(2)
Cu(1)-N(3)	2.0	2.061(2)
Cu(1)-X(1)	2.3	2.4564(13)
Cu(1)-X(1a)	2.8	2.9393(16)
Cu(1)···Cu(1a)[a]	3.6	3.7721(27)
N(1)-Cu(1)-N(2)	81	81.38(10)
N(1)-Cu(1)-N(3)	167	168.60(9)
N(2)-Cu(1)-N(3)	90	90.78(10)
N(1)-Cu(1)-X(1)	92	90.59(8)
N(2)-Cu(1)-X(1)	168	166.63(7)
N(3)-Cu(1)-X(1)	95	95.48(8)
N(1)-Cu(1)-X(1a)[a]	103	102.38(8)
N(2)-Cu(1)-X(1a)[a]	100	100.35(8)
N(3)-Cu(1)-X(1a)[a]	88	87.09(7)
X(1)-Cu(1)-X(1a)[a]	91	91.77(5)
Cu(1)-X(1)-Cu(1a)[a]	89	88.23(5)

[a] Symmetry transformation used to generate equivalent atoms:

a is 1-x,-y, 1-z for **1** and -x, -y, 1-z for **2**.

[b] due to the low level of completeness for this structure only approximate values are given here.

Table S2 Selected bond lengths [Å] and angles [°] for $[Cu_2(L^1)_2(\mu_{1,1}\text{-}N_3)_2]$ (**3**).

	Purple crystals	Dark green crystals
Cu(1)-N(1)	1.9658(16)	1.9656(17)
Cu(1)-N(2)	2.0080(16)	2.0108(16)
Cu(1)-N(20)	2.0157(15)	2.0258(16)
Cu(1)-N(3)	2.0442(15)	2.0597(17)
Cu(1)-N(20a)	2.4111(16)	2.4180(17)
N(20)-N(21)	1.203(2)	1.196(2)
N(21)-N(22)	1.155(3)	1.158(3)
Cu(1)···Cu(1a)[a]	3.3626(4)	3.4116(5)
N(1)-Cu(1)-N(2)	81.54(7)	81.69(7)
N(1)-Cu(1)-N(20)	93.39(6)	94.56(7)
N(2)-Cu(1)-N(20)	169.01(7)	173.93(7)
N(1)-Cu(1)-N(3)	164.50(6)	165.17(7)
N(2)-Cu(1)-N(3)	90.18(6)	89.77(7)
N(20)-Cu(1)-N(3)	92.42(6)	92.86(7)
N(1)-Cu(1)-N(20a)[a]	103.81(6)	99.20(6)
N(2)-Cu(1)-N(20a)[a]	109.09(6)	105.17(6)
N(20)-Cu(1)-N(20a)[a]	81.54(6)	80.08(6)
N(3)-Cu(1)-N(20a)[a]	91.25(6)	94.71(6)
Cu(1)-N(20)-Cu(1a)[a]	98.46(6)	99.92(6)
N(22)-N(21)-N(20)[a]	178.2(2)	177.5(2)

[a] Symmetry transformation used to generate equivalent atoms for purple crystals: a is -x,-y+1,-z+1; Symmetry transformation used to generate equivalent atoms for dark green crystals: a is 1-x, 1-y, 1-z.

Table S3 Selected bond lengths [Å] and angles [°] for $[CuL^{1a}(\mu\text{-}Br)]_\infty$ (**5**).

Cu(1)-N(1)	1.966(7)
Cu(1)-N(2)	1.996(6)
Cu(1)-N(3)	2.058(7)
Cu(1)-Br(1)	2.4687(10)
Cu(1)-Br(1a)	2.9027(13)
Cu(1)···Br(1b)	3.7801(13)
Cu(1)…Cu(1a)	4.1891(10)
N(1)-Cu(1)-N(2)	81.0(3)
N(1)-Cu(1)-N(3)	172.2(3)
N(2)-Cu(1)-N(3)	91.8(3)
N(1)-Cu(1)-Br(1)	91.68(18)
N(2)-Cu(1)-Br(1)	162.0(2)
N(3)-Cu(1)-Br(1)	94.38(18)
N(1)-Cu(1)-Br(1a)	93.7(2)
N(2)-Cu(1)-Br(1a)	98.57(19)
N(3)-Cu(1)-Br(1a)	90.33(18)
Br(1)-Cu(1)-Br(1a)	98.27(3)
N(1)-Cu(1)-Br(1b)	94.4(2)
N(2)-Cu(1)-Br(1b)	85.93(19)
N(3)-Cu(1)-Br(1b)	82.01(18)
Br(1)-Cu(1)-Br(1b)	78.24(3)
Br(1a)-Cu(1)-Br(1b)	171.25(4)
Cu(1)-Br(1)-Cu(1b)	102.20(4)
Cu(1)-Br(1)-Cu(1a)	81.26(3)
Cu(1b)-Br(1)-Cu(1a)	171.25(4)

[a] Symmetry transformations used to generate equivalent atoms:

a is 1-x, y-1/2,-z and b is 1-x,y+1/2,-z.